Supplemental Information

Inhibition of TGF−β signaling in subchondral bone mesenchymal stem cells attenuates osteoarthritis

Gehua Zhen, Chunyi Wen, Xiaofeng Jia, Yu Li, Janet L. Crane, Simon C. Mears, Frederic B. Askin, Frank J. Frassica, Weizhong Chang, Jie Yao, Tariq Nayfeh, Carl Johnson, Dmitri Artemov, Qianming Chen, Zhihe Zhao, Xuedong Zhou, Andrew Cosgarea, John Carrino, Lee Riley, Paul Sponseller, Mei Wan, William Weijia Lu and Xu Cao*

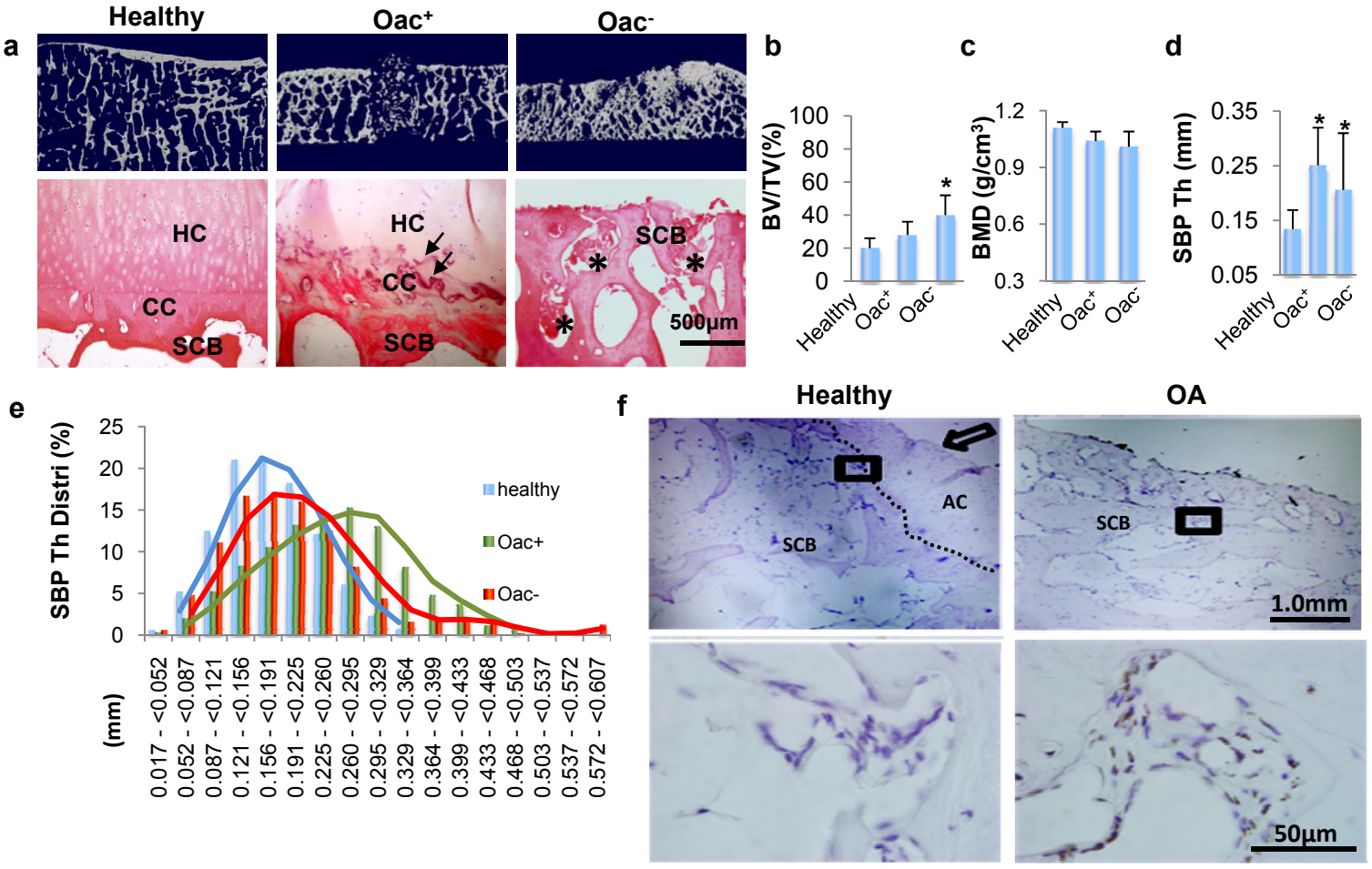

Supplemental Figure 1. Characterization of human knee joints with OA. (**a**) Representative 3D reconstructed μCT images (top panel) and H&E staining (bottom panel) of cross-section of subchondral bone medial compartment. The coronal view in the top panel demonstrates increased bone volume and disrupted bone structure in OA patients compared to healthy controls. Consistent with μCT scanning results, hyaline cartilage (HC) was decreased over OA subchondral bone. At the same time, calcified cartilage (CC) and subchondral bone (SCB) moved toward articular cartilage, and articular cartilage was totally lost at the late stages of OA. Double tide marks are indicated by arrows. (**b-d**) Quantitative analysis of structural parameters of subchondral bone from μCT analysis: bone volume/tissue volume (BV/TV) (**b**), bone mineral density (BMD) (**c**), and average subchondral bone plate thickness (SBP Th) (**d**). BV/TV increased at the sites where cartilage was worn out (Oac$^-$). BMD was not significantly increased parallel the to bone volume fraction, indicating that the newly formed bone was less mineralized. The average SBP Th was greater in OA samples compared to healthy controls, regardless of the presence of articular cartilage. (**e**) Percent distribution of SBP Th (SBP Th Distr). The increased thickness of the SBP in OA samples was not uniform. Consistent with the result shown in panel **(e)**, the SBP generally became thicker as evidenced by a right shift in the distribution curves in the OA samples. (**g**) Immunohistochemical analysis of pSmad2/3 in tibia subchondral bone. Consistent with increased levels of active TGFβ1 in OA subchondral bone, pSmad2/3$^+$ cell number was also increased in OA subchondral bone. n = 10; *P < 0.05; **P < 0.01 vs. healthy. Oac$^+$: OA subchondral bone covered with cartilage, Oac$^-$: OA subchondral bone without cartilage.

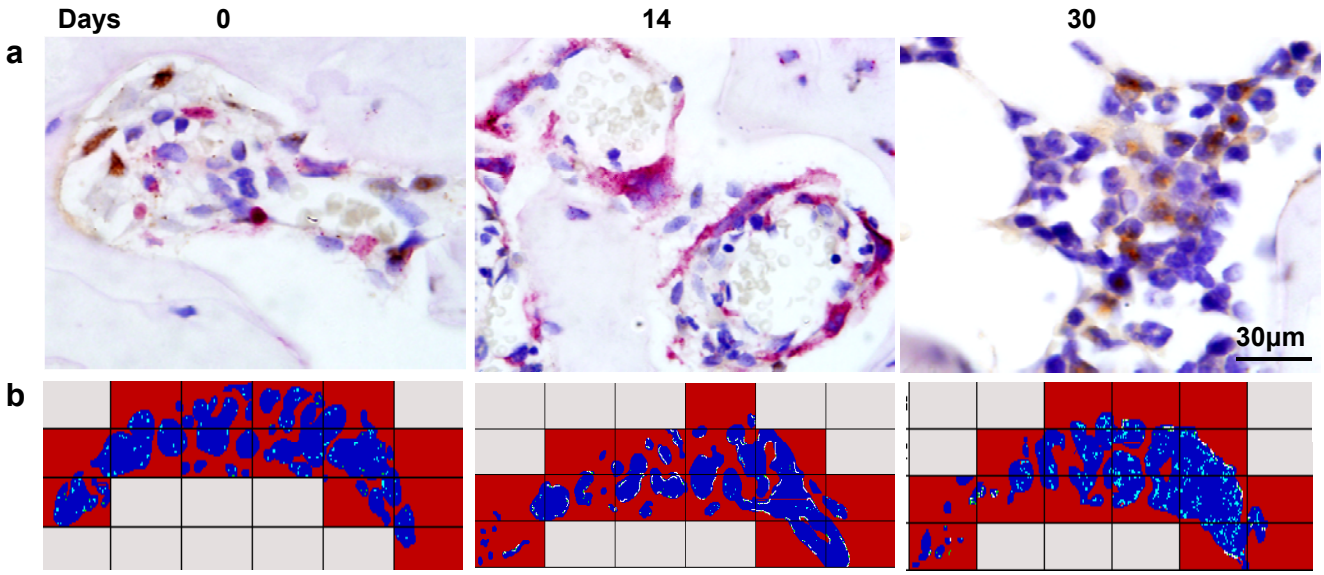

Supplemental Figure 2: Distribution of osterix-positive cells in bone marrow of tibial subchondral bone in ACLT osteoarthritis mouse model. (a) Representative images of immunohistochemical analysis of TRAP (red) and osterix (brown) staining in bone marrow area of tibial subchondral bone in ACLT OA mouse model at 0 (left column), 14 (middle column), and 30 days (right column) after ACLT surgery. **(b)** Histomorphometry analysis atlas of overall distribution of osterix and TRAP positive cells in bone marrow of tibial subchondral bone. TRAP positive cells (osteoclasts) represent the bone remodeling surface and are indicated as white lines; osterix-positive cells are indicated as green dots. As compared with those in Day 0, osteoclasts were increased at day 14 and reduced to baseline by Day 30; in contrast, osterix-positive cells were increased in tibial subchondral bone marrow at Day 30. *n* = 8.

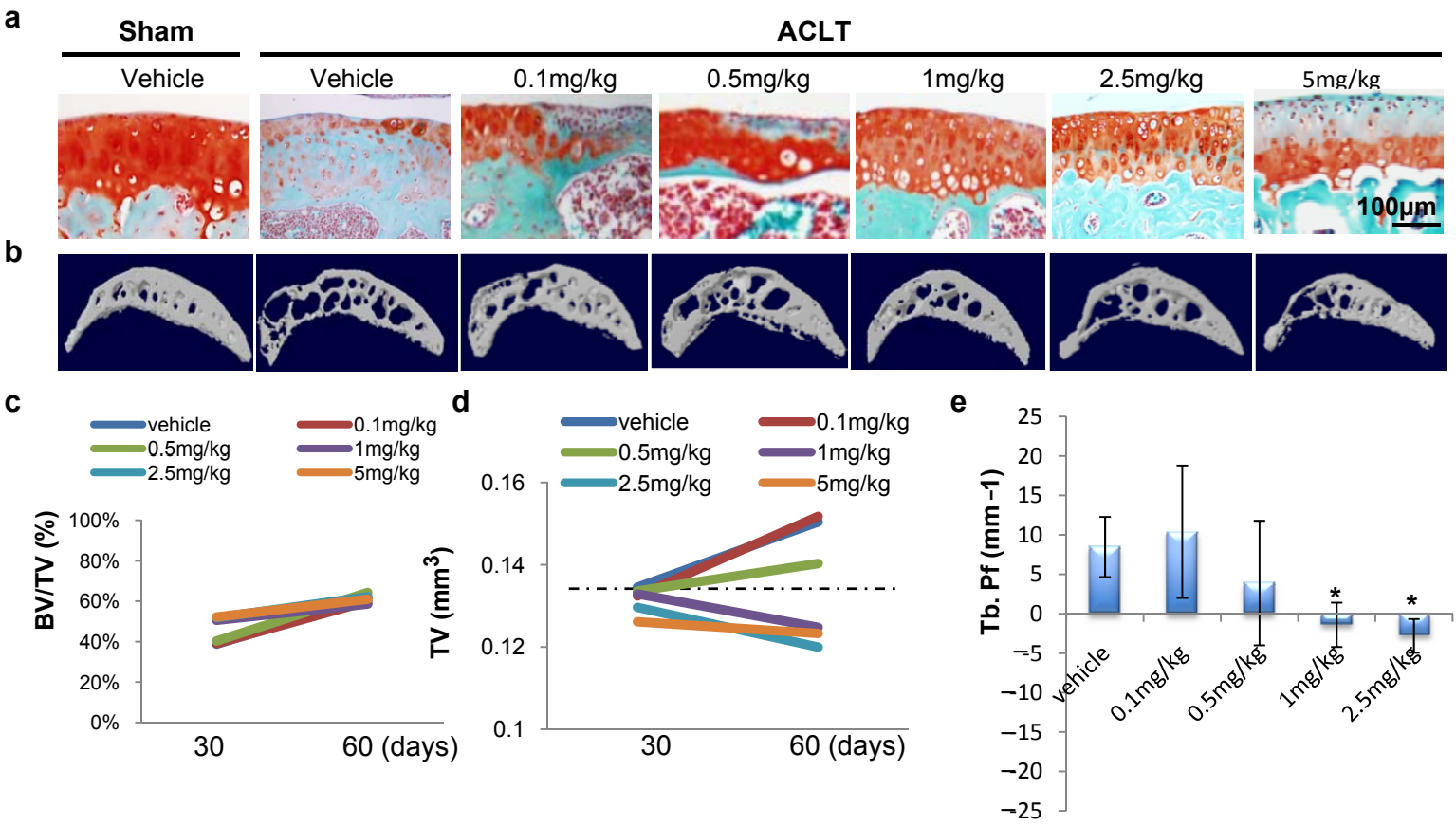

Supplemental Figure 3: Type I TGFβ1 receptor (TβRI) inhibitor dose dependent effects on articular cartilage and subchondral bone. (**a)** Safranin O staining of tibia articular cartilage and adjacent subchondral bone of knee joints from ACLT mice treated with different doses of TβRI inhibitor 2 month after ACLT surgery. (**b**) 3D reconstructed μCT images of subchondral bone of knee joints from ACLT. (**c-e**) Quantitative analysis of μCT parameters of subchondral bone at 30 and 60 days post ACLT surgery: bone volume/tissue volume (BV/TV) (**c**), tissue volume (TV) (**d**), and trabecular pattern factor (Tb. Pf) (**e**). Dotted line indicates the average TV at 30 days post ACLT. Sham-operated mice maintained articular cartilage and subchondral bone structure. In contrast, the ACLT mice treated with vehicle lost most of articular cartilage and had altered subchondral bone morphology. TβRI inhibitor of 1 mg/kg rescued the subchondral bone changes and prevented the degeneration of articular cartilage. Lower doses (0.1 and 0.5 mg/kg) of inhibitor did not completely rescue bone structure, nor prevent the degeneration of articular cartilage. Higher doses (2.5 and 5 mg/kg) of inhibitor could rescue the bone structure but also caused deleterious effects on the articular cartilage, likely because TGFβ1 signaling is essential for maintenance of the articular cartilage. While treatment with the inhibitor did not change BV/TV (**c**), treatment with high doses of the inhibitor (1, 2.5, and 5 mg/kg) inhibited the increase in TV (**d**) and decreased Tb. Pf induced by ACLT surgery (**e**). n = 10, *P < 0.05 vs. vehicle group.

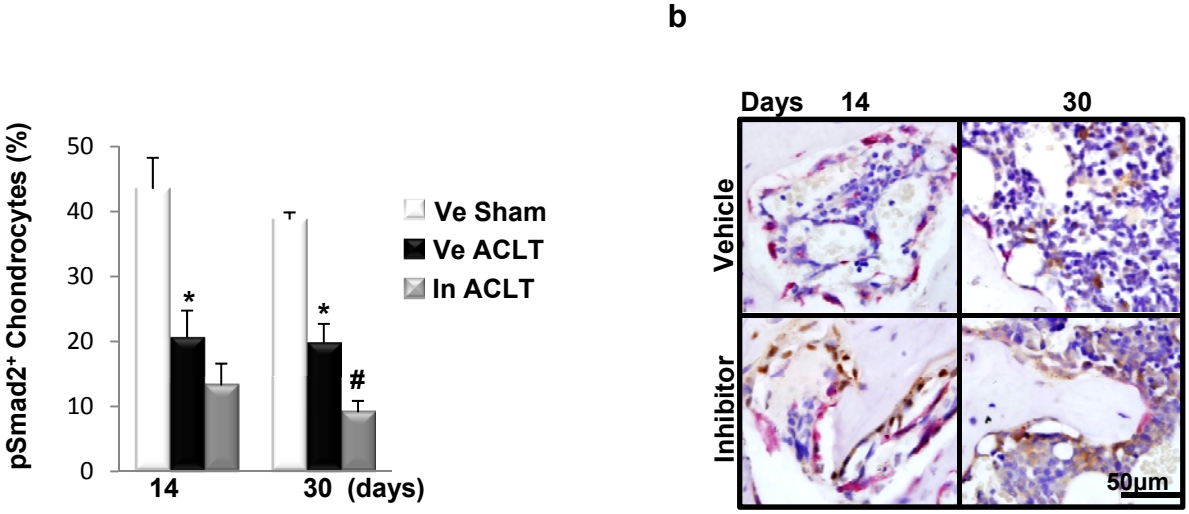

Supplemental Figure 4: Effect of TβRI inhibitor treatment on cartilage TGFβ downstream signaling and subchondral bone remodeling in ACLT mice. (**a**) Quantitative analysis of pSmad2^{+} in chondrocytes of tibial articular cartilage in sham treated with vehicle (Ve Sham) or ACLT mice treated with vehicle (Ve ACLT) or TβRI inhibitor (In ACLT) at 14 or 30 days post surgery. The percentage of pSmad2^{+} chondrocytes significantly decreased post ACLT whereas TβRI inhibitor treatment further reduced the proportions of pSmad2/3^{+} chondrocytes. n = 8, $^{*}P < 0.05$, $^{**}P < 0.01$ vs. sham, $^{\#}P < 0.05$, vs. Vehicle. (**b**) Immunostaining demonstrated that osterix^{+} osteoprogenitors (brown) did not co-localize with TRAP^{+} osteoclasts (pink) in ACLT-Vehicle treated mice (top panels at 14 and 30 days). However, co-localization of osterix and TRAP was seen in ACLT-TβRI inhibitor treated mice (bottom panels). n = 8.

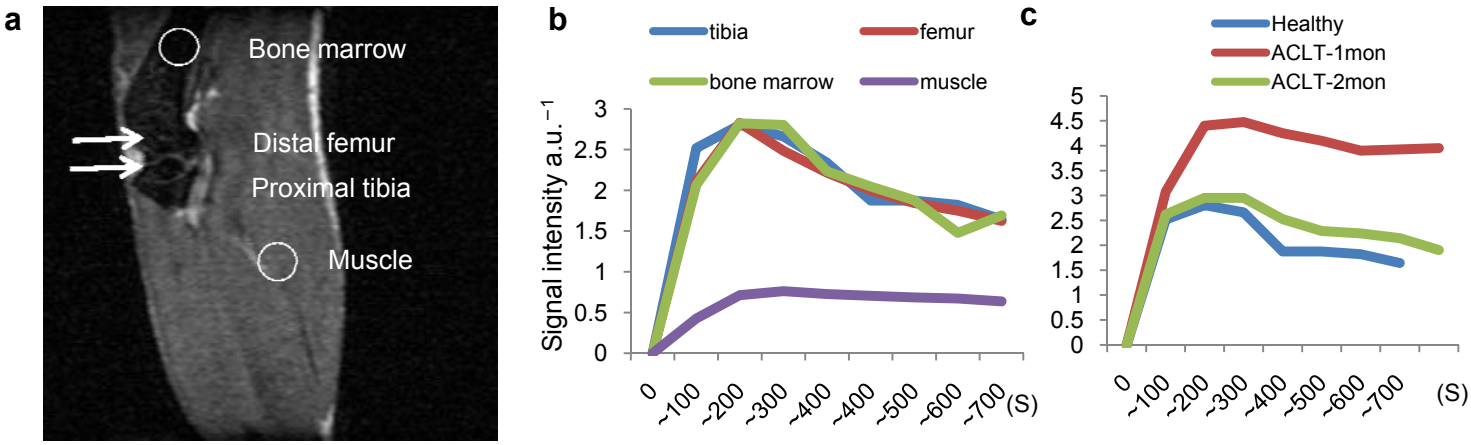

Supplemental Figure 5: Perfusion of subchondral bone of ACLT mice. (**a**) Representative MRI T2 weighted image of knee joint from ACLT mice. (**b**) Validation of the perfusion measurement. Perfusion rates at different sites (marked in (**a**)) in subchondral bone were quantified. As showed in (**b**), the perfusion rates were high in tibia, femur and bone marrow where blood was well supplied. The perfusion rates were low in muscle where blood supply was low. **(c)** Perfusion in subchondral bone of ACLT mice was significantly increased at 1 month, then decreased close to, but still higher than, healthy subchondral bone by 2 months after ACLT surgery. *n* = 8.

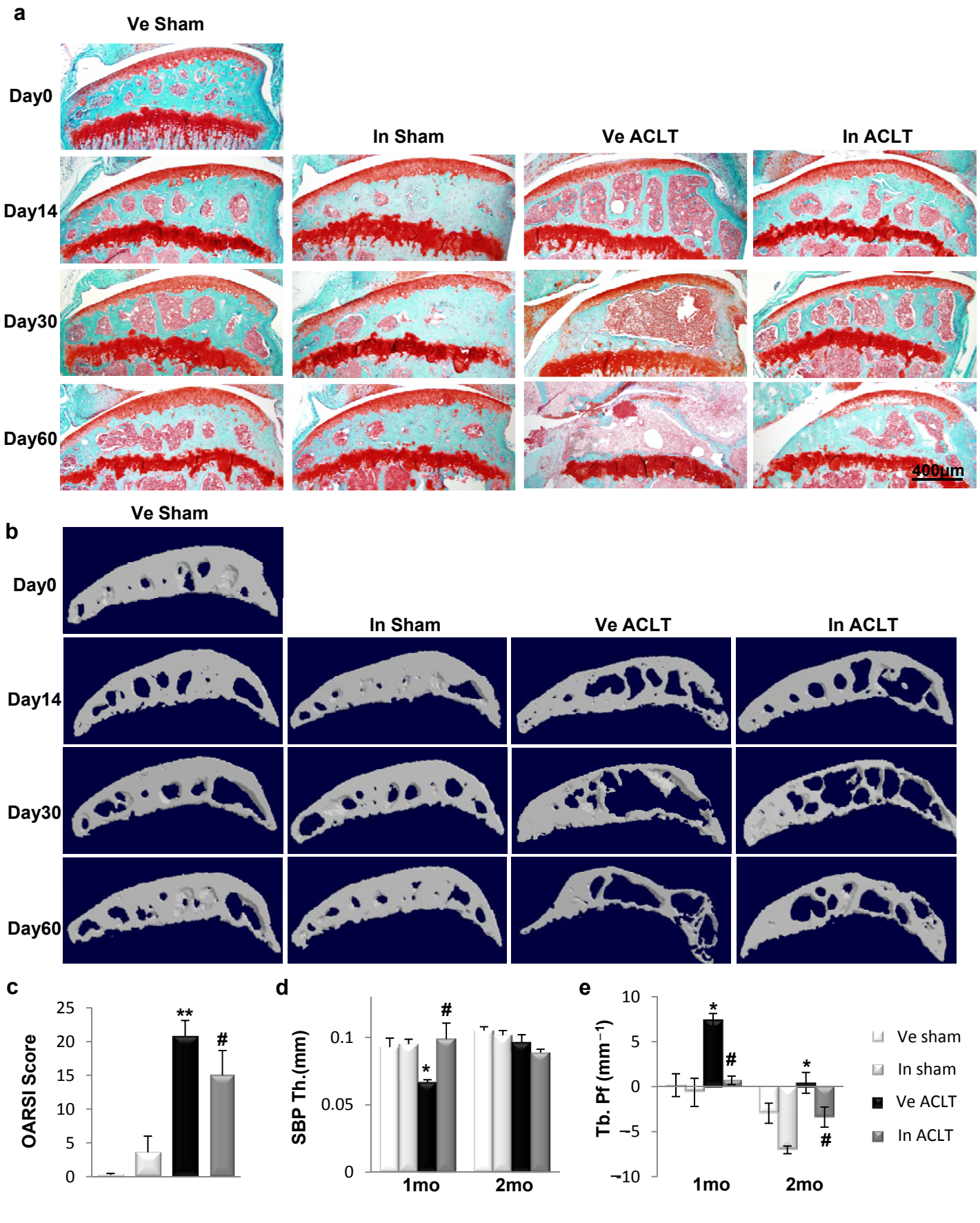
a
Ve Sham
In Sham
Ve ACLT
In ACLT
Day0
Day14
Day30
Day60
400um
b
Ve Sham
In Sham
Ve ACLT
In ACLT
Day0
Day14
Day30
Day60
c
OARSI Score
25
20
15
10
5
0
**
#
d
SBP Th.(mm)
0.1
0.05
0
*
#
1mo
2mo
e
Tb. Pf (mm⁻¹)
10
5
0
−5
−10
*
#
*
#
1mo
2mo
Ve sham
In sham
Ve ACLT
In ACLT

Supplemental Figure 6: TβRI inhibitor treatment improved subchondral bone architecture and attenuated articular cartilage degeneration in 9 month old mice. (**a**) Safranin O staining of tibia articular cartilage and subchondral bone of mice sacrificed at 0, 14, 30, and 60 days post sham or ACLT surgery and treated with either vehicle or TβRI inhibitor (SB505124 - 1mg/kg) daily beginning 3 days post surgery for 1 month. For those mice analyzed at earlier time points, the mice were treated until sacrificed. (**b**) 3D μCT images of subchondral bone of knee joints. The sham-operated mice maintained articular cartilage and subchondral bone structure throughout the duration of the experiment. TβRI inhibitor treatment in sham-operated mice did not have significant effect on articular cartilage and only a slight increase in subchondral bone volume fraction. The degeneration of articular cartilage and disrupted subchondral bone morphology and structure in vehicle treated ACLT mice significantly progressed over 2 months. TβRI inhibitor treatment improved subchondral bone architecture and attenuated the articular cartilage degeneration compared to the ACLT-Vehicle treated mice at similar time points. (**c**) OARSI score based on the histology analysis. (**d-e**) Quantitative analysis of structural parameters by μCT analysis: thickness of subchondral bone plate (SBP, **d**) and trabecular pattern factor (Tb. Pf, **e**). The thickness of the subchondral bone plate was decreased in ACLT-Vehicle treated mice at 1 month post surgery, but remained normal in the ACLT-inhibitor treated mice compared to the sham-operated controls. TβRI inhibitor treatment also decreased the trabecular pattern factor relative to ACLT-Vehicle treated mice at 1 and 2 months post ACLT indicating improvement in bone micro-architecture and connectivity. n = 8, $^{**}P < 0.01$ vs. vehicle sham, $^{\#}P < 0.05$ vs. vehicle ACLT. Ve-Sham: vehicle treated in sham operated; In-Sham: TβRI inhibitor treat in sham operated; Ve-ACLT: vehicle treated in ACLT operated; In-ACLT: TβRI inhibitor treated in ACLT operated mice.

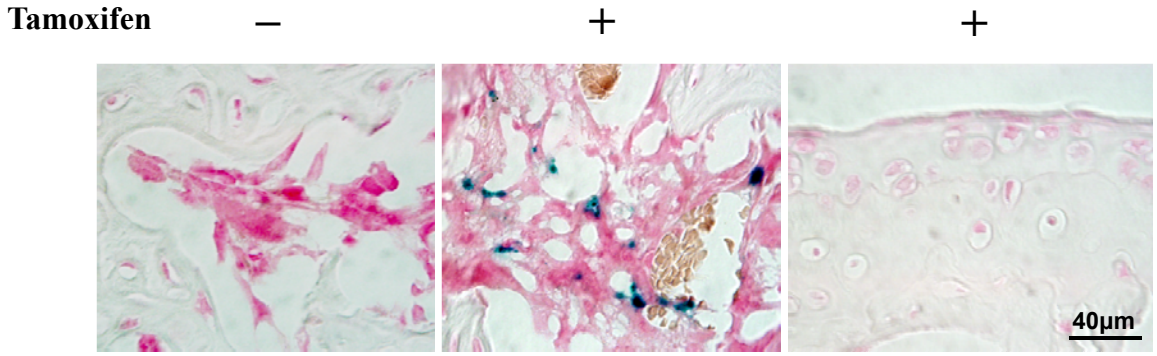

Supplemental Figure 7: β-gal positive cell distributions in tibial subchondral bone and articular cartilage of *Nestin-CreER::Rosa26-lacZ*$^{fl/fl}$ mice 1 month post ACLT surgery. Mice homozygous for the *Gtrosa26tm1Sor* targeted mutation were used to test the cellular expression pattern of the Nestin-Cre transgene. Once induced by tamoxifen, Cre expression results in the removal of a loxP-flanked stop sequence that prevents expression of a lacZ gene. Therefore, X-gal staining for LacZ (blue) is permanently expressed in Nestin-Cre expressing cells and their daughter populations. β-gal positive cells were detected in subchondral bone marrow cavity (2nd panel) but not detected in the articular cartilage after tamoxifen induction 1mo post ACLT (3rd panel). n = 8.

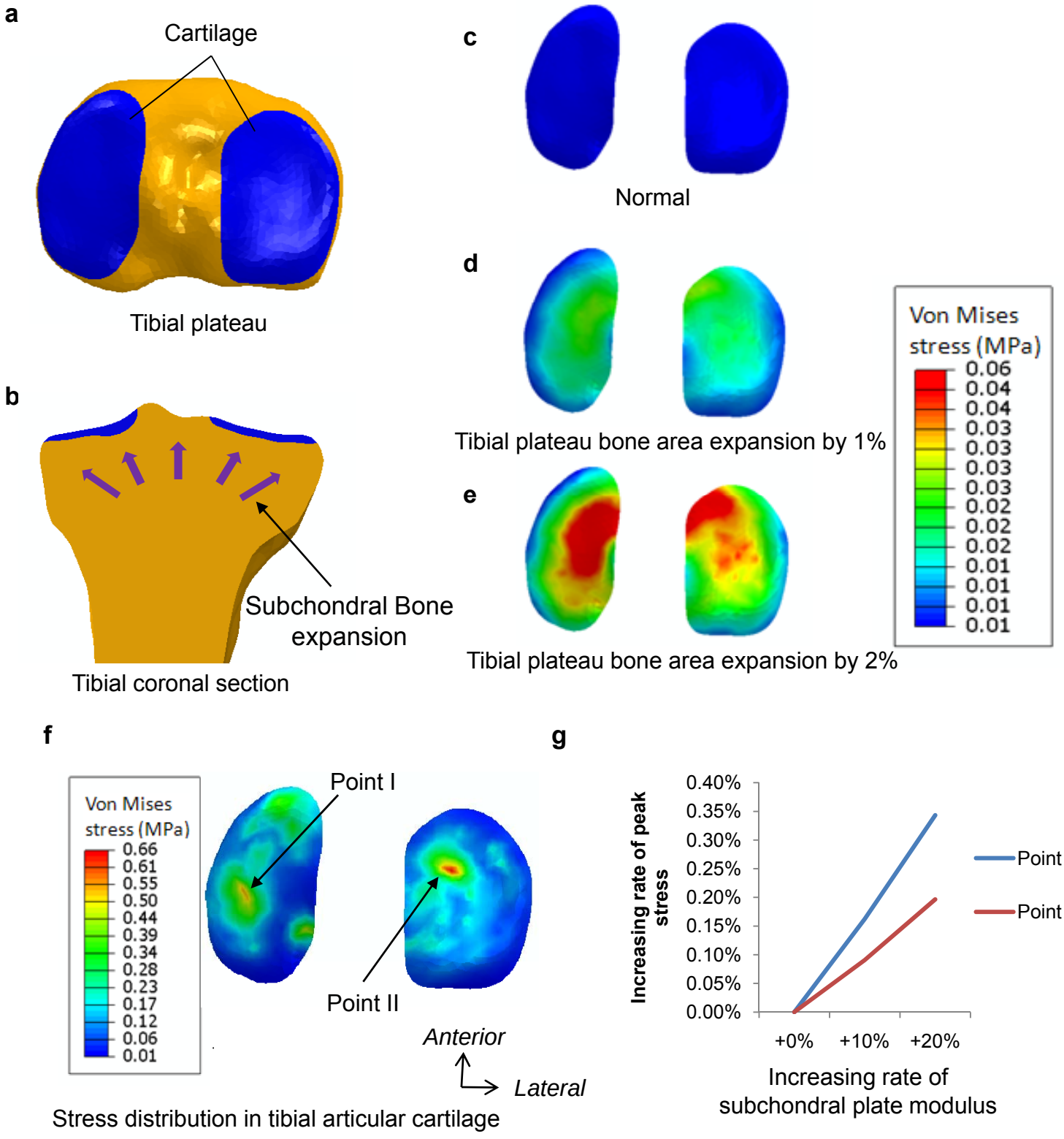

Supplemental Figure 8: Computerized simulation of articular cartilage stress distribution changes with subchondral bone expansion or subchondral bone material properties in human tibia. (**a-b**) An established FE model of human tibial plateau was used for simulation. The subchondral bone size expansion is simulated based on previously published data from large-scale clinical OA studies[1-3] in order to predict overlying articular cartilage stress distribution changes. (**c-e**) As compared with the normal situation (**c**), an incremental increase of 1% (**d**) or 2% (**e**) in subchondral bone size will lead to a significant increase in the stress of articular cartilage.

(**f**) The stress distribution in human articular tibial cartilage with the normal subchondral stiffness modulus under dynamic compression loading of body weight[4]. Point I is the peak stress in the medial condyle articular cartilage; Point II is the peak stress in lateral condyle. (**g**) According to previously published data of bone mineral density with OA progression[3], it is estimated that the increment of subchondral plate stiffness modulus by 10% or 20% will result in significant increase in peak stress on articular surface for both medial and lateral condyles.

References:

1.Frobell, R.B.*, et al.* Presence, location, type and size of denuded areas of subchondral bone in the knee as a function of radiographic stage of OA - data from the OA initiative. *Osteoarthritis Cartilage* **18**, 668-676 (2010).

2.Ding, C., Cicuttini, F. & Jones, G. Tibial subchondral bone size and knee cartilage defects: relevance to knee osteoarthritis. *Osteoarthritis Cartilage* **15**, 479-486 (2007).

3.Dore, D.*, et al.* Subchondral bone and cartilage damage: a prospective study in older adults. *Arthritis Rheum* **62**, 1967-1973 (2010).

4.Choi, K., Kuhn, J.L., Ciarelli, M.J. & Goldstein, S.A. The elastic moduli of human subchondral, trabecular, and cortical bone tissue and the size-dependency of cortical bone modulus. *J Biomech* **23**, 1103-1113 (1990).